

Intramolecular Axial Ligation of Zinc Porphyrin Cores with Triazole Links within Dendrimers

Mutsumi Kimura,^{*,[a, b]} Yasuhiro Nakano,^[a] Naoya Adachi,^[a] Yoko Tatewaki,^[b] Hirofusa Shirai,^[b] and Nagao Kobayashi^[c]

Abstract: A series of dendritic porphyrins **7–9** and **12**, in which benzyl ether dendrons were linked to a porphyrin core through 1,2,3-triazole links, were synthesized by Cu^I-catalyzed cycloaddition of azides and alkynes. Absorption and fluorescence spectra showed a stable axial ligation at the zinc center of the porphyrin core by triazole links in dendritic wedges and in-

dicated that the position of the triazole links strongly affected the stability of the axial ligation within the dendrimer. When the porphyrin core was surrounded by aryl ether dendrons having anionic termini and triazole linkers, a

significant rate enhancement for photo-induced electron transfer was observed compared with a similar water-soluble dendritic zinc porphyrin lacking triazole linkers. These triazole links constituted a direct pathway within the dendrimer architecture for electron transfer between the zinc porphyrin core and peripheral electron acceptors.

Keywords: axial ligation · dendrimers · porphyrins · zinc

Introduction

Biological systems including enzymes, hemoglobin and plant photosynthesis^[1] have provided much of the inspiration for the development of supramolecular devices. Many supramolecular devices have been designed to mimic nanostructures and their functions in biological processes.^[2] These biological systems are generally made up of polypeptide chains; their amino acid sequence determine the structure and function of the resulting protein, which is folded into a unique conformation giving a globular nanostructure incorporating surface clefts and crevices. The special functions in biological systems occur by three-dimensional interactions of molecular units within the globular nanostructures involving hydrophobic effects, hydrogen-bonding, ion–ion interactions

and other forms of intermolecular interactions. Dendrimers have recently been counted among the most attractive macromolecular compounds from the synthetic, structural and functional points of view.^[3] Construction of dendrimers from a functional core results in their isolation from the effects of self-association interactions, sterically shielding them from the external medium and tuning of their surrounding microenvironment. Porphyrins and their metal complexes have been used to a probe of microenvironmental changes by the encapsulation within dendritic structures.^[4] Several studies investigating the dendritic effects of embedding porphyrins in a dendrimer core on their functionalities have reported the use of such systems as synthetic models of natural analogues. For example, Dandliker et al. have reported the construction of a hydrophobic dendrimer having water-soluble terminal segments emanating from an iron(III)–porphyrin core, forming an isolated and water-soluble heme analogue.^[5] Comparison of dendritic iron porphyrins of different dendrimer generations revealed a remarkable shift to positive potential in the redox potential for the Fe³⁺/Fe²⁺ couple of the iron porphyrin core. Aida et al. have reported the dependence of intramolecular energy transduction on the morphology of spherical aryl ether dendritic porphyrins that mimicked biological light-harvesting antennae.^[6]

Three-dimensional interactions between a heme core and peptide side chains have a strong influence on the functionalities such as redox, catalytic, photochemical and molecular recognition properties. Axial ligation at the metal center

[a] Prof. Dr. M. Kimura, Y. Nakano, N. Adachi
Department of Functional Polymer Science
Faculty of Textile Science and Technology, Shinshu University
Ueda 386-8567 (Japan)
Fax: (+81)268-51-5499
E-mail: mkimura@shinshu-u.ac.jp

[b] Prof. Dr. M. Kimura, Dr. Y. Tatewaki, Prof. Dr. H. Shirai
Collaborative Innovation Center of Nanotech Fiber (nanoFIC)
Shinshu University, Ueda 386-8567 (Japan)

[c] Prof. Dr. N. Kobayashi
Department of Chemistry, Graduate School of Science
Tohoku University, Sendai, 980-8587 (Japan)

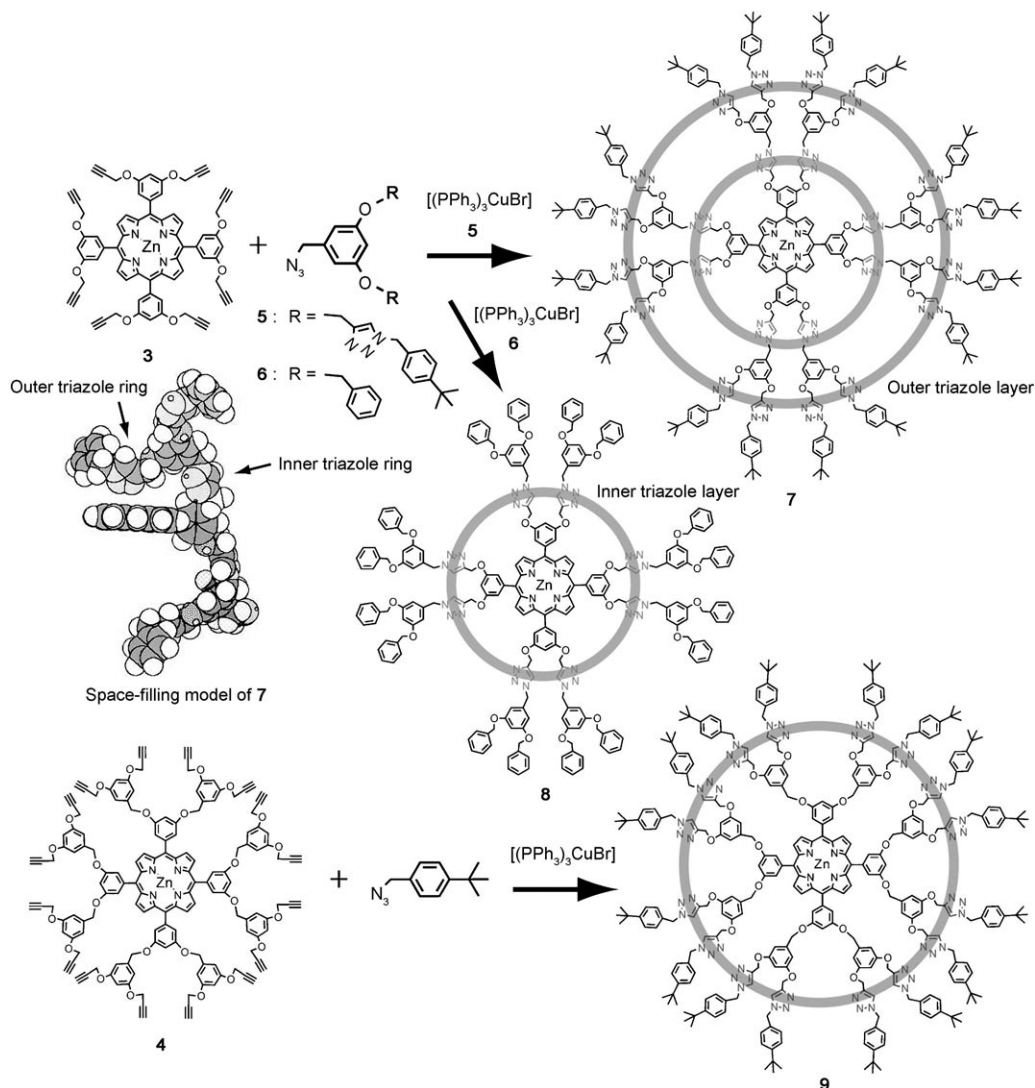
with coordinative imidazole or thiol units in histidine and cysteine, respectively, enhances the functionalities of natural biological systems. Weyermann et al. have reported the creation of a unique local microenvironment around an site-isolated iron porphyrin core by the wrapping the core with a dendrimer in conjugation with axial ligation by imidazoles to mimic electron-transfer proteins such as cytochrome c.^[7] However, three-dimensional interactions between the porphyrin core and the dendritic wedges have not been as extensively explored. We report here the syntheses of the dendritic porphyrins **7–9** containing coordinative 1,2,3-triazole rings using “click chemistry”^[8] for the coupling of acetylene-terminated porphyrin cores with dendritic azides.^[9] Cu^I-catalyzed cycloaddition of azides and alkynes has been widely demonstrated to be a versatile tool in the design and synthesis of materials.^[10] Ornelas et al. have demonstrated the selective recognition of H₂PO₄⁻ and ATP²⁻ in triazole-containing metal dendrimers.^[11] We also discuss the structural dependence of the intramolecular formation of a coordination bond of the zinc porphyrin core with triazole-containing dendrons and the efficiency of photoinduced electron transfer rate.

Results and Discussion

A series of dendritic metalloporphyrins having different dendron units was synthesized by the formation of 1,2,3-triazole links between a porphyrin core and dendritic wedges through a “click reactions”—the Huisgen 1,3-dipolar cycloaddition of azides and acetylenes (Scheme 1).^[12] Alkaline-mediated coupling of 5,10,15,20-tetrakis (3',5'-dihydroxyphenyl)porphyrin with propargyl bromide gave a multivalent porphyrin core **1**, which was metalated with Zn(OAc)₂. Triazole-linked dendritic azide **5** was synthesized by the copper(I)-catalyzed click reaction between *tert*-butyl benzyl azide and 3,5-bis(propargyloxy)benzyl chloride in a mixture of water and *tert*-butyl alcohol, followed by treatment with NaN₃.^[9] Finally, the coupling of the dendritic azide **5** to zinc porphyrin core **3** in THF in the presence of the organosoluble catalyst [(PPh₃)₃CuBr]^[9] yielded the desired dendritic porphyrin **7**, which contained 24 1,4-disubstituted 1,2,3-triazole links in two layers. Metal-free dendritic porphyrin could not be prepared from the coupling between **1** and **5** with [(PPh₃)₃CuBr] due to the metallation of porphyrin cores with copper ions. Purification of **7** was accomplished by column chromatography followed by recycling preparative HPLC and was unambiguously characterized by means of matrix-assisted laser desorption/ionization time-of-flight mass spectra (MALDI-TOF-MS), gel-permeation chromatography (GPC), and ¹H and ¹³C NMR spectroscopy. Analysis of **7** by MALDI-TOF-MS and GPC provided no signs of products with defects and confirmed that the coupling of eight terminal alkynes in **3** and a focal azidomethyl group in **5** is complete. ¹H NMR resonances of the inner triazole units nearer the porphyrin core were shifted downfield compared to those of the outer triazole units, revealing the suc-

cessive generations of a layered structure. The dimensions of the synthesized dendrimer **7** were estimated from the analysis of a surface pressure versus area (π/A) isotherm on pure water as the subphase.^[13] The surface pressure began to rise at a molecular area of about 9 nm², increasing to 35 mNm⁻¹ on further compression. The limiting surface area per molecule of **7** was estimated at 7.8 nm² determined by extrapolating the slope of the π/A isotherm in the liquid-condensed region to zero pressure. The estimated diameter (3.2 nm) of spherical dendrimer **7** almost coincided with the dendrimer diameter (3.5 nm) predicted by computer-generated molecular model. The other dendritic porphyrins **8**, in which the first-generation dendron was linked with the porphyrin core through eight triazole rings in one layer, was synthesized by the coupling between **3** and benzyl ether dendritic azide **6** in a similar manner. While both dendritic porphyrins **7** and **8** contained 28 benzene rings each, the number and position of the triazole links in these molecules were different.

The incorporation of triazole rings in the dendrimer framework may have affected the internal environment around the zinc porphyrin core. Absorption and fluorescence spectra provided information on the internal environment within the dendritic porphyrins. Figure 1 shows the absorption spectra of **7** and **8** in CH₂Cl₂ and toluene at 20 °C. The absorption maxima of the Soret band (λ_{max}) and molar extinction coefficient (ϵ) of **3**, **4**, **7** and **8** in CH₂Cl₂ are summarized in Table 1. In CH₂Cl₂, the Soret and Q bands of **8** (423, 549, 588 nm) were similar to those of the porphyrin core **3** (421, 548, 584 nm), while the Soret band (432 nm) of **7** with its double layer of triazole links in dendritic wedges was red-shifted by 11 nm from that of **3**. Neither the both Soret nor Q bands in **7** and **8** shifted upon increasing the concentration up to 60 μM , indicating the lack of intermolecular aggregation among porphyrin cores in this concentration range. The spectral shift of **7** suggested the formation of intramolecular coordination bonds between the zinc porphyrin core and the triazole links in the dendritic wedges.^[14] Furthermore, in toluene, a broadening and hypochromicity of the Soret band were observed for **7**. The Soret band of **8** was split into two peaks at 430 and 438 nm indicating an equilibrium between coordinated and free species. The position of the triazole links within the dendrimer and the polarity of the environment strongly influenced the stability of triazoles axial ligated to the zinc porphyrin core. To investigate the most favorable positions within the dendrimer of triazole links for the axial ligation, **9** was synthesized by the coupling of acetylene-terminated **4** with *tert*-butyl benzyl azide. Whereas **9** contained the same number of benzene and triazole rings as **8**, the triazole links in **9** were in the outer layer of the dendritic structure. The dendritic porphyrin **9** exhibited the Soret band at 431 nm and Q bands at 559 and 600 nm in CH₂Cl₂, and its absorption peaks for **9** coincided in position with those of **7**, indicating that the triazole links in the outer layer of dendritic wedges could form a stable coordination bond with the zinc porphyrin core.



Scheme 1. Synthetic approach to a series of triazole-linked dendritic porphyrins.

Table 1. Spectroscopic and photophysical data for zinc porphyrin cores and dendritic zinc porphyrins.

	Absorption ^[a] , λ_{max}/nm ($\log \epsilon/M^{-1} cm^{-1}$)	Emission ^[b] , λ_{max}/nm (τ/ns)	$\phi_f^{[c]}$
3	421 (5.76)	598, 645 (1.61)	0.02
4	423 (5.68)	597, 644 (1.58)	0.02
7	432 (5.77)	609, 661 (1.51)	0.02
8	423 (5.73)	597, 645 (1.59)	0.02
9	431 (5.66)	607, 660 (1.61)	0.02

Interactions within the dendrimer could also be monitored by tracking change in fluorescence spectra. Figure 2 shows steady-state fluorescence spectra of **7**, **8** and **9** in degassed CH_2Cl_2 upon the excitation at the Soret band of the porphyrin core. The fluorescence parameters for all dendritic porphyrins and porphyrin cores are also summarized in Table 1. The fluorescence of dendritic porphyrins showed a normal decay profile and the fluorescence lifetime (τ) and

quantum yield (Φ_f) of the porphyrin cores were independent of structural differences in the dendron units. These results suggested that the dendrons exerted little influence of the dendrons on the non-radiative and radiative processes of the porphyrin core. When excited at the Soret band in CH_2Cl_2 , **3**, **4** and **8** emitted at 598 and 645 nm, with the fluorescence intensity ratio I_{598}/I_{645} of about 0.5. On the other hand, **7** and **9** emitted at 609 and 661 nm upon the excitation at the Soret band with a ratio I_{609}/I_{661} of 1.19. The shift in fluorescence peaks and the change in intensity ratio also indicated the formation of intramolecular coordination bonds between the zinc porphyrin core and triazole-containing dendron wedges. The fluorescence spectrum of **8** in toluene was similar to that of **7** and **9**, suggesting the formation of axial ligation in low-polar solvents. These changes in the absorption and fluorescence spectra of **7** and **9** were attributable to the axial ligation of the outer 1,2,3-triazole links in the dendritic wedges to the zinc porphyrin core.

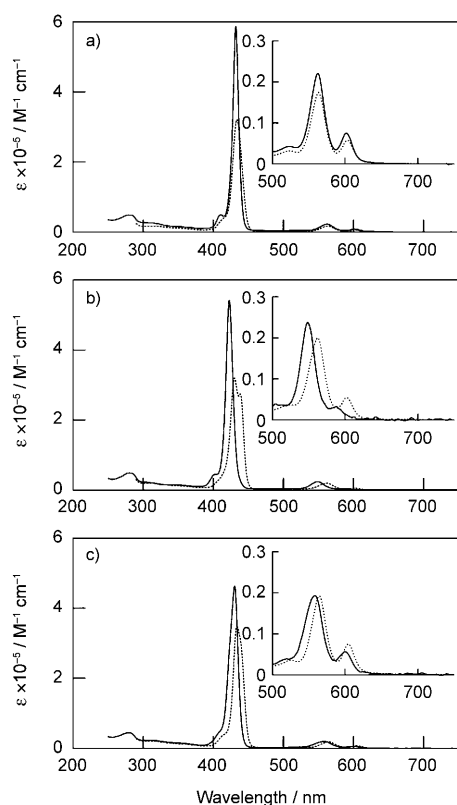


Figure 1. Absorption spectra of dendritic porphyrins a) **7**, b) **8** and c) **9** in CH_2Cl_2 (—) and toluene (.....) at 20 °C. [**7**, **8**, **9**] = 3.0 μM .

The stability of axial ligation in such dendrimers is evaluated by titration with imidazole, which is small enough to penetrate within the dendritic architecture and coordinates strongly to the zinc cation of the porphyrin core. If the triazole links were coordinated to the zinc cation, complexation by imidazole would need an exchange process and the binding constant K would be diminished. The absorption spectrum of **8** in CH_2Cl_2 changed upon titration with imidazole, and isosbestic points were clearly seen (Figure 3). Moreover, the fluorescence spectra changed upon the titration with imidazole as shown in the inset of Figure 3. Titration of **8** with imidazole using Job's method indicated the formation of a 1:1 complex. The constant K was determined from the spectral change in the Soret band. This K value for **8** was $1.9 \times 10^4 \text{ M}^{-1}$, which was comparable to that for non-dendritic zinc porphyrins **3** and **4** (**3**: $K = 1.4 \times 10^4 \text{ M}^{-1}$, **4**: $K = 2.4 \times 10^4 \text{ M}^{-1}$). In sharp contrast, **7** showed no spectral changes in the absorption or fluorescence spectra after the addition of a large excess of imidazole. The titration of **9** with imidazole resulted in a small red shift of the Soret band from 431 to 434 nm and a small change in the intensity ratio of the two peaks in fluorescence spectra at high imidazole concentration. These titration results indicated that the stability of axial ligation strongly depended on the spatial position of the triazole rings within the dendritic structure and on the distance between the zinc cation and these rings. A computer-generated model of **7** predicted the distances of the tria-

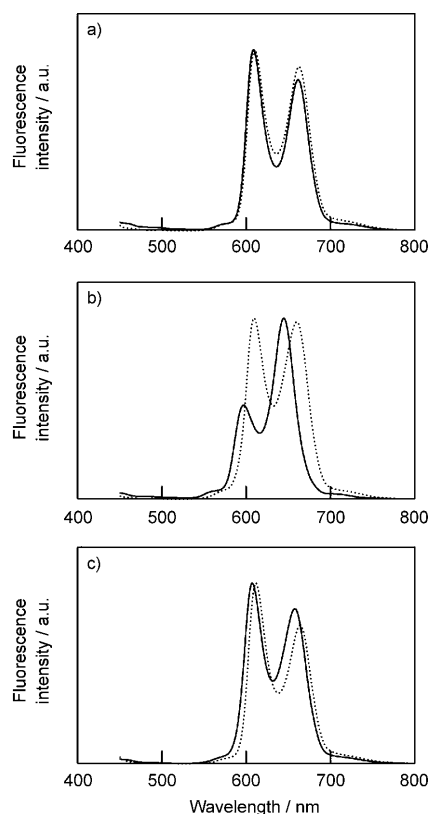


Figure 2. Steady-state fluorescence spectra of dendritic porphyrins a) **7**, b) **8** and c) **9** upon excitation at the Soret band at 20 °C in CH_2Cl_2 (—) and toluene (.....). All spectra are normalized to a constant absorbance at the excitation wavelength.

zole links in each layer of the dendritic structure as shown in Scheme 1. The approach of the inner triazoles to the porphyrin core was difficult due to the covalent linkages at the 3- and 5-positions of phenyl ring bound to the porphyrin core. On the other hand, the flexibility of the dendritic wedge allowed the formation of coordination bond between the outer triazole links and the porphyrin core.

In natural heme proteins like cytochrome c, chlorophyll, hemoglobin and metal-containing enzymes, metalloporphyrins are buried within the hydrophobic peptide shell through the formation of coordination bonds with the coordinative side chains of surrounding peptides.^[1] Such wrapping of porphyrins with peptide shell provides a suitable environment for various functionalities. Spectral studies of triazole-containing dendritic porphyrins have clearly demonstrated that the dendritic wedges create a unique microenvironment around the zinc porphyrin core. The axial ligation of triazole links may affect the functionalities of the zinc porphyrin core. In the electron-transfer process in natural cytochrome, the histidine units in the globular protein shell provide the pathway for electron transfer between two redox sites.^[15] The triazole links in the dendrimer are good mimics of the protein histidine residue in the biotic systems. We focus on the change in photochemical properties of the zinc-porphyrin core upon wrapping with triazole-containing wedges.

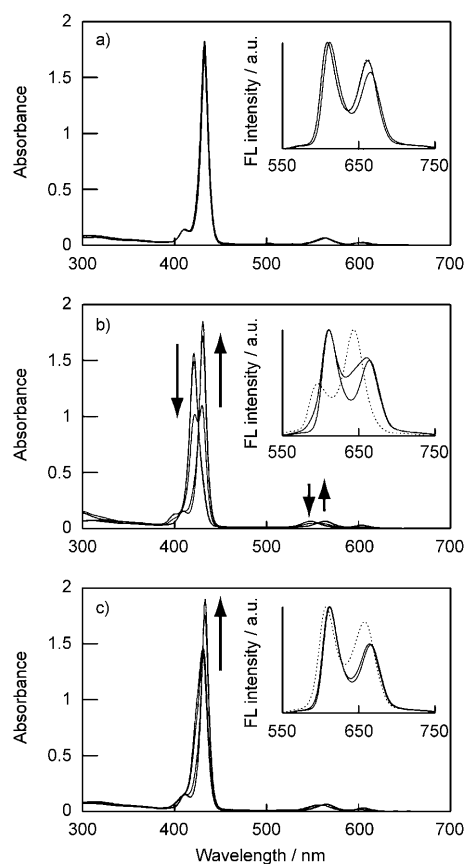
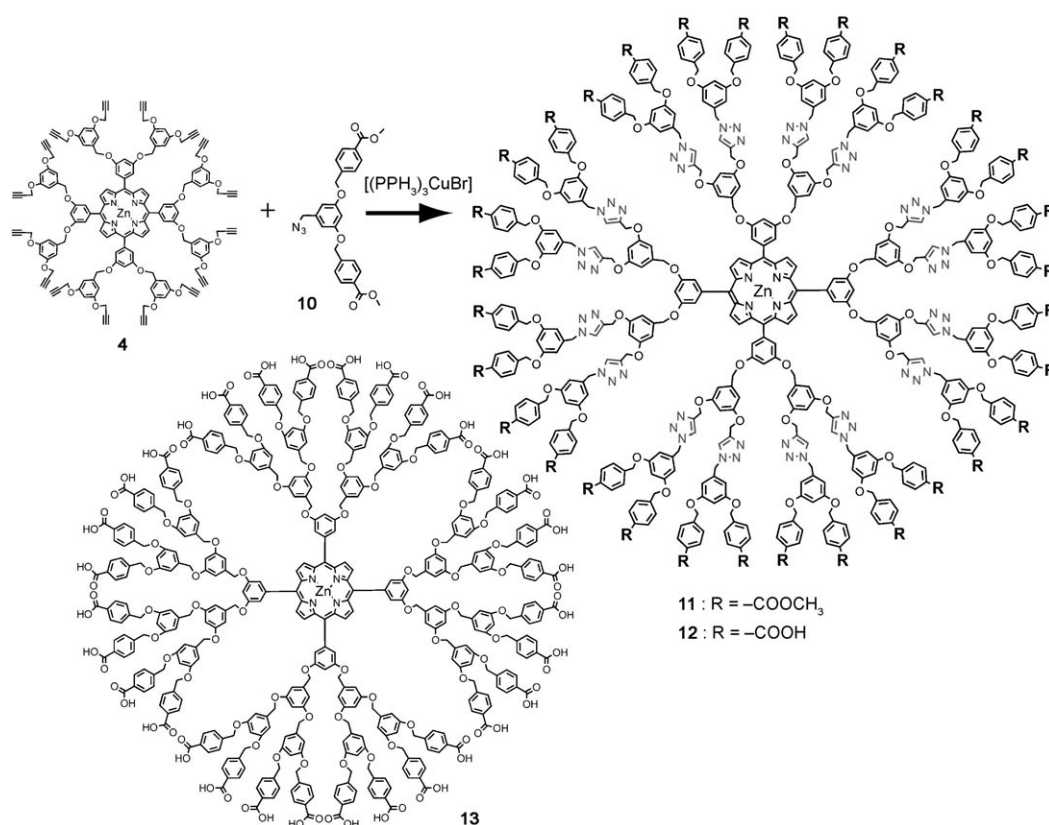


Figure 3. Absorption changes of a) **7**, b) **8** and c) **9** in CH_2Cl_2 at 20°C on titration with imidazole. [**7**, **8**, **9**] = $3.0\ \mu\text{M}$. [imidazole] = 0, 1.0, 10.0, 100.0, 1000 μM . The inset shows fluorescence spectral changes of a) **7**, b) **8** and c) **9** in CH_2Cl_2 at 20°C on titration with imidazole; [**7**, **8**, **9**] = $3.0\ \mu\text{M}$; [imidazole] = 0 (.....), 10.0, 1000 μM .

Water-soluble dendritic zinc porphyrin **12** was synthesized by the Cu^1 -catalyzed coupling reaction between **4** and methoxycarbonyl-terminated aryl ether dendritic azide **10**, followed by hydrolysis of the exterior ester groups with KOH (Scheme 2).^[16] The absorption spectrum of **12** in alkaline aqueous solution (pH 10.7) exhibited the Soret band at 435 nm and the Q bands at 563 and 603 nm. Water-soluble dendritic zinc porphyrin **12** emitted at 607 and 660 nm upon the excitation at the Soret band with intensity ratio $I_{607}/I_{660} = 1.26$. These absorption and fluorescence spectra were similar to those obtained for **9** in CH_2Cl_2 , suggesting the formation of intramolecular axial ligation of triazole links with the zinc-porphyrin core in aqueous solution. Self-assembled donor-acceptor systems have shown promise for the generation of long-lived charge-separated species through photoinduced electron transfer and charge separation processes.^[17,18] Aida and co-workers have demonstrated the long-range photoinduced electron transfer through an aryl ether dendrimer framework in a water-soluble dendritic zinc porphyrin.^[16] In this system, the cationic electron acceptor methyl viologen (MV^{2+}) accumulated on the surface of anionic surface of a dendrimer and the fluorescence from the zinc por-

phyrin core was quenched through the photoinduced electron transfer through the dendrimer framework. We examined the photoinduced electron transfer from the excited zinc porphyrin core in **12** to MV^{2+} in aqueous solution. Methyl viologen is a typical one-electron transfer acceptor unit producing the methyl viologen radical.^[19] The addition of MV^{2+} up to 20 mM to **12** did not change the zinc porphyrin absorption bands. This result is in accord with the titration behavior of the reference dendritic zinc porphyrin **13** lacking the triazole links.^[16] Therefore, the absence of spectral change in **12** upon addition of MV^{2+} revealed that the dendritic wedges prevent access of MV^{2+} to the zinc porphyrin core.

The fluorescence decreased in intensity upon titration with MV^{2+} . The relative fluorescence intensity at 607 nm is plotted as a function of MV^{2+} concentration (Figure 4). Fluorescence quenching processes are described by the Stern-Volmer equation ($I_0/I = K_{\text{SV}}[\text{MV}^{2+}] + 1$), where $K_{\text{SV}} = k_q\tau_0$, K_{SV} is the Stern-Volmer quenching constant (M^{-1}), k_q is the quenching rate constant ($\text{M}^{-1}\text{s}^{-1}$), and τ_0 is the excited singlet lifetime of the zinc porphyrin in the absence of a quencher. The Stern-Volmer plots of **12** showed a highly efficient fluorescence quenching at a low concentration of MV^{2+} . The initial slope of the Stern-Volmer plots gave the Stern-Volmer quenching constant $K_{\text{SV}} = 1.54 \times 10^5 \text{M}^{-1}$ and k_q was $9.6 \times 10^{13} \text{M}^{-1}\text{s}^{-1}$. This value of k_q was much higher than the diffusion-limited rate constant in water ($k_d = 7.6 \times 10^9 \text{M}^{-1}\text{s}^{-1}$) for neutral species calculated by the Smoluchowski equation,^[20] indicating the accumulation of MV^{2+} around **12** through electrostatic forces. In sharp contrast, the reference dendrimer **13** showed the saturation of I_0/I at concentration of MV^{2+} above 0.2 mM.^[16] The rate of photoinduced electron transfer depends on the thermodynamic driving force for the electron-transfer reactions, the nature of intervening medium, and the distance and relative orientation of the donor and the acceptor.^[21] While **12** was larger than that of **13** due to the presence of triazole links within the dendritic wedges,^[22] the efficiency of electron transfer in **12** was higher than that in **13**. Our findings may be rationalized by considering that the increase in quenching efficiency of **12** was attributed to the triazole links within the dendritic wedges. These links constitute an electron transfer pathway from the excited zinc-porphyrin core buried in the dendrimer to MV^{2+} accumulated on the dendrimer surface. A mixed solution of **12** and MV^{2+} exhibited the characteristic absorption bands at 305 and 602 nm in the presence of triethanolamine as a sacrificial donor under the irradiation with visible light.^[23] Furthermore, these spectral changes disappeared when the sample was subsequently exposed to O_2 . These observations are consistent with the formation of the methyl viologen radicals. This result implied that the triazole-linked dendritic porphyrin **12** acted as a photosensitizer in this artificial photosynthetic system.



Scheme 2. Water-soluble dendritic zinc porphyrins **12** and **13**.

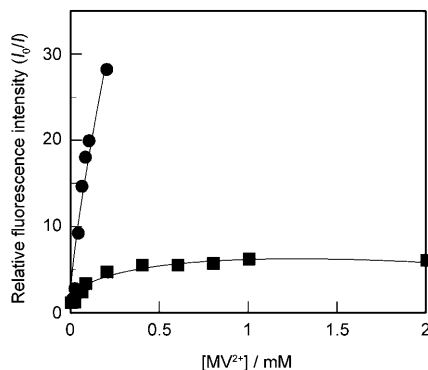


Figure 4. Stern–Volmer plots for fluorescence quenching of **12** (●) and **13** (■) with MV²⁺ in degassed alkaline aqueous solution at pH 10.7. The fluorescence intensity was monitored at 607 and 660 nm for **12** and **13**, respectively, [**12**, **13**] = 1.5 μM.

Conclusion

Novel triazole-linked dendritic porphyrins have been synthesized though the click reaction between acetylene-terminated porphyrin and dendritic azides. Absorption and fluorescence spectroscopic studies demonstrated the binding ability of the triazole links to bind as axial ligands for the zinc porphyrin core within the single dendrimer. We also found that the binding ability depended on the spatial posi-

tion of these links in the dendritic architecture. The axial ligation affected the efficiency of photoinduced electron transfer from the excited zinc porphyrin core to an electron acceptor. The construction of triazole-containing dendritic wedges around the porphyrin core allowed the creation of a unique microenvironment and the coordination of triazole links created an electron transfer pathway from core to periphery within each dendrimer. The design of interactive dendron wedges^[11,24] could control the properties of the functional core and a well-designed dendrimer could serve as a good mimic of the natural bio-systems involved in photosynthesis, oxygen transportation and catalysis. By covalently inserting the interactive segments in the dendrimer, the functional tuning of the porphyrin core could be further extended in future work.

Experimental Section

General: NMR spectra were recorded on a Bruker AVANCE 400 FT NMR spectrometer at 399.65 MHz and 100.62 MHz for ¹H and ¹³C, respectively, in CDCl₃ solution. Chemical shifts are reported relative to internal TMS. IR spectra were obtained on a SHIMADZU IR Prestige-21 with DuraSample IR II. UV/Vis spectra and fluorescence spectra were measured on a JASCO V-650 and a JASCO FP-750. Fluorescence quantum efficiencies were determined by HAMAMATSU Photonics absolute PL Quantum Yield Measurement system C9920-02. MALDI-TOF mass spectra were obtained on a PerSeptive Biosystems Voyager-De-Pro spec-

trometer with dithranol as matrix resolution GPC analyses were carried out with a JASCO HPLC system (pump 1580, UV detector 1575, refractive index detector 930) and a Showa Denko GPC KF-804 L column (8.0×300 mm, polystyrene standards, $M_w = 900\text{--}400\,000\text{ g mol}^{-1}$) in THF as an eluent at 35 °C (1.0 mL min⁻¹).

Materials: Dendritic azides **5**, **6**, **10** and water-soluble dendritic zinc porphyrin **13** were synthesized from dendritic halides according to the literature method.^[16,25] All chemicals were purchased from commercial suppliers and used without purification. Column chromatography was performed with activated alumina (Wako, 200 mesh) or Wakogel C-200. Recycling preparative gel permeation chromatography was carried out by a JAI recycling preparative HPLC using CHCl₃ as an eluent. Analytical thin-layer chromatography was performed with commercial Merck plates coated with silica gel 60 F₂₅₄ or aluminum oxide 60 F₂₅₄.

Porphyrin core 1: 5,10,15,20-Tetrakis(3',5'-dihydroxyphenyl)porphyrin (80.0 mg, 0.11 mmol) and propargyl bromide (0.1 mL, 1.31 mmol) were dissolved in acetone (10 mL) containing K₂CO₃ (0.36 g, 2.61 mmol) and [18]crown-6 (catalytic amount), and the reaction mixture was refluxed for 3 d with stirring. The mixture was filtrated and the filtrate was evaporated to dryness. The crude product was purified using column chromatography (activated alumina, petroleum ether/CH₂Cl₂ 1:1). Yield: 84 mg, 73%. ¹H NMR (400 MHz, CDCl₃): δ = 8.95 (s, 8H, pyrrole), 7.52 (s, 8H, ArH), 7.04 (s, 4H, ArH), 4.86 (s, 16H, -O-CH₂-C=CH), 2.59 (s, 8H, -O-CH₂-C=CH), -2.84 ppm (s, 2H, -NH); ¹³C NMR (100 MHz, CDCl₃): δ = 56.3 (-O-CH₂-C=CH), 75.9 (-C=CH), 78.4 (-C=CH), 102.3, 115.4, 119.4 (porphyrin), 144.0, 156.8 ppm; MALDI-TOF-MS: *m/z*: calcd for C₆₈H₄₆N₄O₈: 1047.12 [*M*+H]⁺; found 1047.3; UV/Vis (CH₂Cl₂): λ_{max} (log ε) = 420 (5.73), 514 (4.46), 548 (4.10), 589 (4.08), 646 nm (3.91).

Porphyrin core 2: Prepared from 5,10,15,20-tetrakis(3',5'-dihydroxyphenyl)porphyrin and 3,5-bis(propargyloxy)benzyl chloride and purified by column chromatography (activated alumina, petroleum ether/CH₂Cl₂ 1:1). Yield: 60 mg, 38%. ¹H NMR (400 MHz, CDCl₃): δ = 8.83 (s, 8H, pyrrole), 7.47 (s, 8H, ArH), 7.04 (s, 4H, ArH), 6.67 (s, 16H, ArH), 6.60 (s, 8H, ArH), 5.20 (s, 16H, -CH₂O-), 4.64 (s, 32H, -O-CH₂-C=CH), 2.38 (s, 16H, -O-CH₂-C=CH), -2.92 ppm (s, 2H, -NH); ¹³C NMR (100 MHz, CDCl₃): δ = 55.9 (-O-CH₂-C=CH), 70.0 (-CH₂O-), 75.8 (-C=CH), 78.3 (-C=CH), 102.3, 106.9, 115.3, 119.6 (porphyrin), 139.4, 144.0, 157.8, 158.9 ppm; MALDI-TOF-MS: *m/z*: calcd for C₁₄₈H₁₁₀N₄O₂₄: 2328.74 [*M*+H]⁺; found 2329.1; UV/Vis (CH₂Cl₂): λ_{max} (log ε) = 422 (5.71), 516 (4.34), 551 (3.85), 589 (4.08), 646 (3.91).

Zinc porphyrin core 3 and 4: A mixture of **1** or **2** (50.0 mg, 47.8 μmol) and Zn(OAc)₂·2H₂O (16.0 mg, 71.6 μmol) were dissolved in acetic acid (5 mL). During the reaction, UV/Vis spectrum of the reaction mixture was monitored. The mixture was refluxed until no change in the Soret band was observed. After aqueous workup (50 mL), the mixture was extracted with CH₂Cl₂ and the organic layer was washed with water for 3 times. The organic layer was dried (MgSO₄) and evaporated. The residue was purified by chromatography on activated alumina with CH₂Cl₂ to afford the zinc porphyrin core.

Compound 3: Yield: 42 mg, 80%; ¹H NMR (400 MHz, CDCl₃): δ = 9.03 (s, 8H, pyrrole), 7.48 (s, 8H, ArH), 6.99 (s, 4H, ArH), 4.79 (s, 16H, -O-CH₂-C=CH), 2.57 ppm (s, 8H, -O-CH₂-C=CH); ¹³C NMR (100 MHz, CDCl₃): δ = 56.2 (-O-CH₂-C=CH), 75.9 (-C=CH), 78.4 (-C=CH), 102.3, 115.4, 120.4 (porphyrin), 144.7, 156.8 ppm; MALDI-TOF-MS: *m/z*: calcd for C₆₈H₄₄N₄O₈Zn: 1110.49 [*M*]⁺; found 1109.0; UV/Vis (CH₂Cl₂): λ_{max} (log ε) = 421 (5.76), 548 (4.39), 584 nm (3.50).

Compound 4: Yield: 109 mg, 95%; ¹H NMR (400 MHz, CDCl₃): δ = 8.86 (s, 8H, pyrrole), 7.35 (s, 8H, ArH), 6.82 (s, 4H, ArH), 6.58 (s, 16H, ArH), 6.45 (s, 8H, ArH), 4.98 (s, 16H, -CH₂O-), 4.51 (s, 32H, -O-CH₂-C=CH), 2.30 ppm (s, 16H, -O-CH₂-C=CH); ¹³C NMR (100 MHz, CDCl₃): δ = 54.9 (-O-CH₂-C=CH), 69.0 (-CH₂O-), 74.7 (-C=CH), 77.3 (-C=CH), 100.8, 105.9, 114.2, 119.5 (porphyrin), 138.3, 148.9, 156.6, 157.8 ppm; MALDI-TOF-MS: *m/z*: calcd for C₁₄₈H₁₁₀N₄O₂₄: 2391.84 [*M*]⁺; found 2389.6; UV/Vis (CH₂Cl₂): λ_{max} (log ε) = 423 (5.68), 549 (4.29), 584 nm (3.38).

General procedure of dendritic porphyrins through click chemistry: A solution of dendritic azide (0.57 mmol), porphyrin core (9.0 μmol), *N,N*-diisopropylethylamine (1.5 μL, 9.0 μmol) and [Cu(PPh₃)₃Br] (2.5 mg,

2.7 μmol) in tetrahydrofuran (10 mL) was heated at 60 °C for 3 d. The residue was purified by column chromatography on silica gel by eluting with CH₂Cl₂ and recycling preparative GPC.

Compound 7: Yield: 29 mg, 53%; ¹H NMR (400 MHz, CDCl₃): δ = 8.79 (s, 8H, pyrrole), 7.59 (s, 8H, ArH), 7.33 (s, 8H, ArH), 7.27 (s, 16H, ArH), 7.23 (d, 32H, *J* = 8.4 Hz, ArH), 7.18 (s, 4H, ArH), 6.99 (d, 32H, *J* = 8.4 Hz, ArH), 6.39 (s, 8H, triazole), 6.35 (s, 16H, triazole), 5.36 (s, 16H, -CH₂O-), 5.21 (s, 32H, -CH₂O-), 5.16 (s, 16H, -CH₂O-), 4.65 (s, 32H, -CH₂O-), 1.20 ppm (s, 144H, *t*Bu); ¹³C NMR (100 MHz, CDCl₃): δ = 31.2, 34.5, 53.7, 107.4, 122.8, 125.9, 127.8, 131.3, 143.3, 151.8, 159.7 ppm; MALDI-TOF-MS: *m/z* calcd for C₃₄₈H₃₇₂N₇₆O₂₄Zn: 6068.56 [*M*]⁺; found 6070.7; UV/Vis (CH₂Cl₂): λ_{max} (log ε) = 432 (5.77), 563 (4.36), 602 nm (3.92).

Compound 8: Yield: 31 mg, 90%; ¹H NMR (400 MHz, CDCl₃): δ = 8.80 (s, 8H, pyrrole), 7.35 (s, 8H, ArH), 7.31 (s, 8H, ArH), 7.15 (m, 96H, ArH), 6.81 (s, 4H, ArH), 6.40 (s, 8H, triazole), 6.27 (s, 16H, -CH₂O-), 5.15 (s, 16H, -CH₂O-), 4.74 ppm (s, 32H, -CH₂O-); ¹³C NMR (100 MHz, CDCl₃): δ = 53.3, 70.0, 72.3, 102.2, 107.1, 123.3, 127.4, 127.9, 128.5, 133.4, 136.3, 142.3, 155.3, 160.2 ppm; MALDI-TOF-MS: *m/z*: calcd for C₂₃₆H₁₉₆N₂₈O₂₄Zn: 3873.64 [*M*]⁺; found 3875.3; UV/Vis (CH₂Cl₂): λ_{max} (log ε) = 423 (5.73), 549 (4.38), 588 nm (3.60).

Compound 9: Yield: 25 mg, 52%; ¹H NMR (400 MHz, CDCl₃): δ = 8.95 (s, 8H, pyrrole), 7.41 (s, 8H, ArH), 7.20 (d, 32H, *J* = 8.4 Hz, ArH), 6.95 (m, 36H, ArH), 6.60 (s, 16H, triazole), 6.40 (s, 8H, ArH), 5.16 (s, 32H, -CH₂O-), 4.95 (s, 16H, -CH₂O-), 4.76 (s, 32H, -CH₂O-), 1.17 ppm (s, 144H, *t*Bu); ¹³C NMR (100 MHz, CDCl₃): δ = 31.2, 34.5, 53.6, 70.1, 106.7, 123.3, 125.9, 127.8, 131.4, 143.75, 151.7, 160.1 ppm; MALDI-TOF-MS: *m/z*: calcd for C₃₂₄H₃₄₈N₅₂O₂₄Zn: 5419.95 [*M*]⁺; found 5420.4; UV/Vis (CH₂Cl₂): λ_{max} (log ε) = 431 (5.66), 559 (4.29), 600 nm (3.75).

Compound 11: Yield: 77 mg, 88%. ¹H NMR (400 MHz, CDCl₃): δ = 8.86 (s, 8H, pyrrole), 7.84 (d, 64H, *J* = 7.6 Hz, ArH), 7.40 (s, 16H, ArH), 7.27 (s, 8H, ArH), 7.22 (d, 32H, *J* = 7.2 Hz, ArH), 6.93 (s, 4H, ArH), 6.63 (s, 16H, triazole), 6.47 (s, 8H, ArH), 6.36 (s, 16H, ArH), 6.27 (s, 32H, ArH), 5.14 (s, 32H, -CH₂O-), 4.98 (s, 16H, -CH₂O-), 4.92 (s, 32H, -CH₂O-), 4.79 (s, 64H, -CH₂O-), 3.77 ppm (s, 96H, -COOCH₃); ¹³C NMR (100 MHz, CDCl₃): δ = 52.0, 53.6, 68.0, 69.2, 102.0, 107.1, 119.3, 126.9, 129.6, 133.9, 136.9, 141.5, 131.4, 159.5, 159.9, 166.6 ppm; MALDI-TOF-MS: *m/z*: calcd for C₅₄₈H₄₇₆N₅₂O₁₂₀Zn: 9775.31 [*M*]⁺; found 9770.9.

Hydrolysis of the exterior ester groups in 11: To a solution of **11** (15 mg, 1.53 μmol) in tetrahydrofuran (5 mL) was added 1.5 M KOH aqueous solution (0.1 mL). The reaction was heated at reflux for 6 h. The reaction mixture was then evaporated to dryness, and water (5 mL) was added resulting in a homogeneous solution, which was then heated for 4 h. After being cooled to room temperature, acetic acid (1 mL) was added to the reaction solution, resulting in a purple suspension, which was collected by centrifugation. The purple precipitate was washed with water (2 mL × 3) and dried overnight in a vacuum oven at 50 °C to afford hydrolyzed dendrimer **12**. Yield: 11 mg, 79%; FT-IR: ν_{max} = 1692 cm⁻¹ (COOH); UV/Vis (pH 10.7 aq KOH): λ_{max} (log ε) = 435 (5.58), 563 (4.22), 603 nm (3.82).

Acknowledgements

This work was supported by a project for "Innovation Creative Center for Advanced Interdisciplinary Research Areas" in Special Coordination Funds for Promoting Science and Technology from the Ministry of Education, Culture, Sports, Science and Technology of Japan. We also thank Prof. M. Ichikawa of Shinshu University for fluorescence lifetime measurements.

- [1] J. A. Cowan, *Inorganic Biochemistry An Introduction*, VCH, New York, 1993.
- [2] J. W. Steed, J. L. Atwood, *Supramolecular Chemistry*, Wiley, New York, 2002.

- [3] a) C. Gorman, *Adv. Mater.* **1998**, *10*, 295; b) A. W. Bosman, H. M. Janssen, E. W. Meijer, *Chem. Rev.* **1999**, *99*, 1665; c) G. R. Newkome, H. He, C. N. Moorefield, *Chem. Rev.* **1999**, *99*, 1689; d) S. Hecht, J. M. J. Fréchet, *Angew. Chem.* **2001**, *113*, 76; *Angew. Chem. Int. Ed.* **2001**, *40*, 74; e) G. E. Oosterom, J. N. H. Reek, P. C. J. Kamer, P. W. N. M. van Leeuwen, *Angew. Chem.* **2001**, *113*, 1878; *Angew. Chem. Int. Ed.* **2001**, *40*, 1828.
- [4] a) P. J. Dandliker, F. Diederich, M. Gross, C. B. Knobler, A. Louati, E. M. Sanford, *Angew. Chem.* **1994**, *106*, 1821; *Angew. Chem. Int. Ed. Engl.* **1994**, *33*, 1739; b) K. W. Pollak, J. W. Leon, J. M. J. Fréchet, M. Maskus, H. D. Abruña, *Chem. Mater.* **1998**, *10*, 30; c) K. W. Pollak, E. M. Sanford, J. M. J. Fréchet, *J. Mater. Chem.* **1998**, *8*, 519; d) M. S. Matos, W. Verheijen, F. C. De Schryver, S. Hecht, K. W. Pollak, J. M. J. Fréchet, B. Forier, W. Dehaen, *Macromolecules* **2000**, *33*, 2967; e) M. Kimura, T. Shiba, M. Yamazaki, K. Hanabusa, H. Shirai, N. Kobayashi, *J. Am. Chem. Soc.* **2001**, *123*, 5636; f) M. Sakamoto, A. Ueno, H. Mihara, *Chem. Eur. J.* **2001**, *7*, 2449; g) S. Van Doorslaer, A. Zingg, A. Schweiger, F. Diederich, *ChemPhysChem* **2002**, *3*, 659; h) M. Kimura, K. Saito, K. Ohta, K. Hanabusa, H. Shirai, N. Kobayashi, *J. Am. Chem. Soc.* **2002**, *124*, 5274; i) O. Finikova, A. Galkin, V. Rozhkov, M. Cordero, C. Hägerhäll, S. Vinogradov, *J. Am. Chem. Soc.* **2003**, *125*, 4882; j) T. Imaoka, R. Tanaka, S. Arimoto, M. Sakai, M. Fujii, K. Yamamoto, *J. Am. Chem. Soc.* **2005**, *127*, 13896; k) S. A. Chavan, W. Maes, L. E. M. Gevers, J. Wahlen, I. F. J. Vankelecom, P. A. Jacobs, W. Dehaen, D. E. De Vos, *Chem. Eur. J.* **2005**, *11*, 6754; l) W.-S. Li, K. S. Kim, D.-L. Jiang, H. Tanaka, T. Kawai, J. H. Kwon, D. Kim, T. Aida, *J. Am. Chem. Soc.* **2006**, *128*, 10527; m) J. Larsen, B. Brüggemann, T. Khoury, J. Sly, M. J. Crossley, V. Sundström, E. Åkesson, *J. Phys. Chem. A* **2007**, *111*, 10589.
- [5] P. J. Dandliker, F. Diederich, J.-P. Gisselbrecht, A. Louati, M. Gross, *Angew. Chem.* **1995**, *107*, 2906; *Angew. Chem. Int. Ed. Engl.* **1995**, *34*, 2725.
- [6] D.-L. Jiang, T. Aida, *J. Am. Chem. Soc.* **1998**, *120*, 10895.
- [7] P. Weyermann, J.-P. Gisselbrecht, C. Boudon, F. Diederich, M. Gross, *Angew. Chem.* **1999**, *111*, 3400; *Angew. Chem. Int. Ed.* **1999**, *38*, 3215.
- [8] H. C. Kolb, M. G. Finn, K. B. Sharpless, *Angew. Chem.* **2001**, *113*, 2056; *Angew. Chem. Int. Ed.* **2001**, *40*, 2004.
- [9] P. Wu, A. K. Feldman, A. K. Nugent, C. J. Hawker, A. Scheel, B. Voit, J. Pyun, J. M. J. Fréchet, K. B. Sharpless, V. V. Fokin, *Angew. Chem.* **2004**, *116*, 4018; *Angew. Chem. Int. Ed.* **2004**, *43*, 3928.
- [10] a) W. G. Lewis, L. G. Green, F. Grynszpan, Z. Radić, P. R. Carlier, P. Taylor, M. G. Finn, K. B. Sharpless, *Angew. Chem.* **2002**, *114*, 1095; *Angew. Chem. Int. Ed.* **2002**, *41*, 1053; b) B. Helms, J. L. Mynar, C. J. Hawker, J. M. J. Fréchet, *J. Am. Chem. Soc.* **2004**, *126*, 15020; c) R. J. Thibault, K. Takizawa, P. Lowenheim, B. Helms, J. L. Mynar, J. M. J. Fréchet, C. J. Hawker, *J. Am. Chem. Soc.* **2006**, *128*, 12084; d) G. K. Such, J. F. Quinn, A. Quinn, E. Tipto, F. Caruso, *J. Am. Chem. Soc.* **2006**, *128*, 9318; e) J. A. Johnson, D. R. Lewis, D. D. Díaz, M. G. Finn, J. T. Koberstein, N. J. Turro, *J. Am. Chem. Soc.* **2006**, *128*, 6564; f) H. Nandivada, H.-Y. Chen, L. Bondarenko, J. Lahann, *Angew. Chem.* **2006**, *118*, 3438; *Angew. Chem. Int. Ed.* **2006**, *45*, 3360; g) T. Devic, O. David, M. Valls, J. Marrot, F. Couty, G. Férey, *J. Am. Chem. Soc.* **2007**, *129*, 12614.
- [11] C. Ornelas, R. Aranzaes, E. Cloutete, S. Alves, D. Astruc, *Angew. Chem.* **2007**, *119*, 890; *Angew. Chem. Int. Ed.* **2007**, *46*, 872.
- [12] R. Huisgen, *1,3-Dipolar Cycloaddition Chemistry* (Ed.: A. Padwa), Wiley, New York, **1984**, pp. 1–176.
- [13] a) Y. Tomoyose, D.-L. Jiang, R.-H. Jin, T. Aida, T. Yamashita, K. Horie, E. Yashima, Y. Okamoto, *Macromolecules* **1996**, *29*, 5236; b) P. Bhyrappa, G. Vaijayanthimala, K. S. Suslick, *J. Am. Chem. Soc.* **1999**, *121*, 262.
- [14] A. P. H. J. Schenning, C. Elissen-Román, J.-W. Weener, M. W. P. L. Baars, S. J. van der Gaast, E. W. Meijer, *J. Am. Chem. Soc.* **1998**, *120*, 8199.
- [15] a) J. J. Regan, B. E. Ramirez, J. R. Winkler, H. B. Gray, B. G. Malmström, *J. Bioenerg. Biomembr.* **1998**, *30*, 35; b) B. E. Ramirez, B. G. Malmström, J. R. Winkler, H. B. Gray, *Proc. Natl. Acad. Sci. USA* **1995**, *92*, 11949; c) H. J. Hwang, Y. Lu, *Proc. Natl. Acad. Sci. USA* **2004**, *101*, 12842.
- [16] R. Sadamoto, N. Tomioka, T. Aida, *J. Am. Chem. Soc.* **1996**, *118*, 3978.
- [17] a) P. Piotrowiak, *Chem. Soc. Rev.* **1999**, *28*, 143; b) T. Hayashi, H. Ogoshi, *Chem. Soc. Rev.* **1997**, *26*, 503.
- [18] a) N. Sutin, *Acc. Chem. Res.* **1982**, *15*, 275; b) P. L. Luisi, M. Giomini, M. P. Pileni, B. H. Robinson, *Biochim. Biophys. Acta Rev. Biomembr.* **1988**, *947*, 209; c) S. M. B. Costa, P. L. Cornejo, D. M. Togashi, C. A. T. Laia, *J. Photochem. Photobiol. A* **2001**, *142*, 151; d) A. Uehara, H. Nakamura, S. Usui, T. Matsuo, *J. Phys. Chem.* **1989**, *93*, 8197; e) F. M. Menger, M. I. Angelova, *Acc. Chem. Res.* **1998**, *31*, 789; f) J. H. Fendler, *Science* **1984**, *223*, 988; g) P. J. G. Coutinho, S. M. B. Costa, *J. Photochem. Photobiol. A* **1994**, *82*, 149; h) R. Rossetti, S. M. Beck, L. Brus, *J. Am. Chem. Soc.* **1984**, *106*, 980; i) V. Ramamurthy, D. F. Eaton, *Acc. Chem. Res.* **1988**, *21*, 300; j) S. Hamai, T. Koshiyama, *J. Photochem. Photobiol. A* **1999**, *127*, 135; k) J. K. Thomas, *Chem. Rev.* **1993**, *93*, 301; l) L. Persaud, A. J. Bard, A. Champion, M. A. Fox, F. E. Mallouk, S. E. Webber, J. M. White, *J. Am. Chem. Soc.* **1987**, *109*, 7309; m) H. Ringsdorf, B. Schlarb, J. Venzmer, *Angew. Chem.* **1988**, *100*, 117; *Angew. Chem. Int. Ed. Engl.* **1988**, *27*, 113; n) A. Harriman, Y. Kubo, J. L. Sessler, *J. Am. Chem. Soc.* **1992**, *114*, 388; o) P. J. F. de Rege, S. A. Williams, M. J. Therien, *Science* **1995**, *269*, 1409; p) D. M. Togashi, S. M. B. Costa, *New J. Chem.* **2002**, *26*, 1774.
- [19] a) J. R. Darwent, P. Douglas, A. Harriman, G. Porter, M.-C. Richoux, *Coord. Chem. Rev.* **1982**, *44*, 83; b) I. Okura, *Coord. Chem. Rev.* **1985**, *68*, 83.
- [20] a) M. V. Smoluchowski, *Z. Phys. Chem. (Leipzig)* **1917**, *92*, 129; b) D. M. Togashi, S. M. B. Costa, *Phys. Chem. Chem. Phys.* **2002**, *4*, 1141.
- [21] a) S. F. Nelsen, D. A. Trieber II, M. A. Nagy, A. Konradsson, D. T. Halfen, K. A. Splan, J. R. Pladziewicz, *J. Am. Chem. Soc.* **2000**, *122*, 5940; b) P. F. Barabara, T. J. Meyer, M. A. Ratner, *J. Phys. Chem.* **1996**, *100*, 5940.
- [22] The limiting surface area per molecule of **11** was 6.5 nm² estimated from the analysis of π/A isotherm.
- [23] a) T. Watanabe, K. Honda, *J. Phys. Chem.* **1982**, *86*, 2617; b) S. Aono, I. Okura, *J. Phys. Chem.* **1985**, *89*, 1593; c) I. Okura, Y. Kinumi, *Bull. Chem. Soc. Jpn.* **1990**, *63*, 2922; d) G. McLendon, D. S. Miller, *J. Chem. Soc. Chem. Commun.* **1980**, 533.
- [24] T. R. Chan, R. Hilgraf, K. B. Sharpless, V. V. Fokin, *Org. Lett.* **2004**, *6*, 2853.
- [25] a) C. J. Hawker, J. M. J. Fréchet, *J. Am. Chem. Soc.* **1990**, *112*, 7638; b) J. W. Leon, M. Kawa, J. M. J. Fréchet, *J. Am. Chem. Soc.* **1996**, *118*, 8847; c) R.-H. Jin, T. Aida, S. Inoue, *J. Chem. Soc. Chem. Commun.* **1993**, 1260.

Received: July 31, 2008
Published online: February 2, 2009